JOURNAL OF SUSTAINABLE MATERIALS PROCESSING AND MANAGEMENT
e-ISSN: 2821-2843

JSMPM

Vol. 5 No. 1 (2025) 76-88
https://publisher.uthm.edu.my/ojs/index.php/jsmpm

Conventional Friction Stir Welding and Bobbin Friction Stir Welding for Joining Space Grade Aluminium Alloy 6061-T6 by an Industry-compatible Way: A Comparative Study

Rawaha Imran Elahi[1], Muhammad Sohail Hanif[1]*, Syed Ahsan Abbas Zaidi[1], Muhammad Taha Siddiqui[1], Bilal Ahmed[1]

[1] *Department of Materials Engineering,*
NED University of Engineering and Technology, Karachi, 75270, PAKISTAN

*Corresponding Author: msohailhanif@neduet.edu.pk
DOI: https://doi.org/10.30880/jsmpm.2025.05.01.008

Article Info

Received: 27 February 2025
Accepted: 25 April 2025
Available online: 14 May 2025

Keywords

6061-T6, Bobbin tool, comparison, friction stir welding, pin tool, tool development

Abstract

Friction Stir Welding (FSW) is a modern solid-state joining process. It joins materials without allowing them to melt, with minimal change in their properties. There are multiple types of FSW based on the method of implementation. In the current study, the two most common techniques of FSW, known as Conventional Friction Stir Welding (CFSW) and Bobbin Friction Stir Welding (BFSW), are employed to fabricate butt joints of space-grade aluminum alloy 6061-T6 by utilizing the conventional milling machine, in-house development of FSW tool and heat treating the high temperature steel (H-13) using low cost steel foil method. Two different types of tools were manufactured, heat treated and FSW was performed. The comparison of the properties attained by the butt joints are presented in this study. Two welds were successful out of four successful experiments performed, which were found to contain an average tensile strength of 128 MPa along with 65-97% of average base metal hardness. It was also concluded that BFSW is more reliable for longer joints.

1. Introduction

Friction Stir Welding (FSW) is a modern solid-state joining process developed in 1991 by The Welding Institute (TWI) [1]. Its first practical application took place in Sapa, Vietnam, in November 1996, where hollow aluminum sheets were used for deep-freezing fisheries [2,3]. Now, more than a decade has passed since FSW began to be widely used in aerospace, aviation, marine industries, fuel tanks, and pipelines [4]. The process creates joints by rotating a non-consumable welding tool on the workpiece, generating heat through friction and plastic deformation, which softens the material and allows the tool to stir the joint [5]. FSW is mainly used to join wrought aluminum alloys from the 2xxx, 5xxx, 6xxx, and 7xxx series, as these alloys are generally considered non-weldable or difficult to weld by fusion welding techniques [6]. Furthermore, FSW provides significantly better properties compared to other welding processes, such as fusion welding, when joining aluminum alloys. This is because it is a solid-state joining process, meaning the material being welded is not allowed to melt and recast [7]. Moreover, it is also an eco-friendly and operator-friendly technique because no protective gases, arcs, smoke and fumes are generated in the process [8,9]. Different variants of FSW are available, among them, the two important types are known as Conventional friction stir welding (CFSW) and Bobbin friction stir welding (BFSW) also known as self-reacting friction stir welding (SR-FSW). These processes are primarily differentiated based on the tool design, as

the BFSW tool contain an additional shoulder as compared to the CFSW tool [10]. The CFSW tool, known as Pin tool consists of a single shoulder with a stationary backing anvil acting as a heat sink [11]. The BFSW tool is known as Bobbin tool or a Self-reacting tool that uses two opposing rotating shoulders (top shoulder and lower shoulder) connected with a fully penetrated pin. The lower shoulder of this tool replaces the backing plate used in the conventional welding process which creates a major effect on heating of workpiece and handling of plasticized material of workpiece [12-14]. It has many advantages as compared to the conventional tools such as the symmetry of thickness, low weld joint distortion, and elimination of root defect in welds [15]. The tool performance is highly dependent on the profile of the pin, welding speed, rotational speed, and tilt angle, all of which influence the mechanical and microstructural properties of the resulting weld [16-18]. Furthermore, the three main issues of Back support, weld thinning and keyhole defects that are commonly encountered in CFSW can be eliminated using BFSW [19].

The 6xxx aluminum alloy series is considered as a good structural material and is extensively used in aerospace industries as a space-grade alloy and automotive industry [20-22]. This 6xxx series accounts for a significant percentage of global aluminum production [23]. The 6061-T6 alloy has attractive properties like high strength-to-weight ratio, formability, fatigue, and corrosion resistance. Many researchers have proposed different tool designs and considerations for the performance of FSW on aluminum alloys. Hoyos and Serna [24] had analyzed around 80 sources and 200 tests to develop a mathematic mode for the selection of optimum shoulder diameter, pin diameter and pin length for pin tool with respect to the thickness and grade of aluminum alloys, Chupradit et al. [25] found that higher pin angle on pin tool reduces heat generation and increases stirring action of tool in the welding process, Fuse and Badheka [26] concluded that the best performance of bobbin tool can be achieved by maintaining the ratio of shoulder to pin diameter of 3. Amin et al. [27] suggested that for the most optimum bobbin tool design the internal diameter of the pin should be similar to the thickness of workpiece, ratio of shoulder diameter to pin diameter should be 3 and the gap between the both shoulders should also be equal to the thickness of workpiece. Furthermore, various shoulder profiles, pin profiles and dimensions along different welding parameters were used by different researchers to perform or simulate CFSW and BFSW [28-34].

In this study, a butt joint of space grade Aluminum alloy AA 6061-T6 was fabricated by utilizing both CFSW and BFSW techniques in the most suitable and cheaper way which can be applicable in almost all fabrication industries and then the properties of joints were compared with each other. This comparative study aims to identify which FSW technique is the most reliable under the currently available industry-friendly resources.

2. Materials and Method

The 3mm thick 6061-T6 aluminum alloy plates (185mm × 95mm) were selected as base metals (BMs) to produce FSW joints. The properties of base metal are shown in Table 1. The Air hardening H13 tool steel rod of 20 mm diameter was used to fabricate both CFSW and BFSW tools.

Table 1 *Mechanical properties of base metal*

Base Metal	Properties			
	Vickers hardness (HV)	Ultimate tensile strength (MPa)	Elongation (%)	Bend strength (MPa)
6061-T6	100	284	14.2	626

2.1 Fabrication of Tools

A non-consumable tapered pin tool Fig. 1(a) with a concave shoulder was fabricated in order to perform CFSW and similarly, a non-consumable cylindrical pin bobbin tool Fig. 1(b) having two flat shoulders of the same diameter was fabricated for the performance of BFSW. Both tools were fabricated by the machining of an H13 rod using a widely used conventional medium duty lathe machine to the required shape and dimensions as shown in Table 2.

Table 2 *Dimensions of tools*

Tool	Tool Dimensions				
	Pin feature (°)	Pin length (mm)	Pin diameter (mm)	Shoulder feature (°)	Shoulder diameter (mm)
Cylindrical Pin Tool	28° tapered	2.7	4.6	8° Concave	13.9
Cylindrical Pin Bobbin Tool	Straight	3	6.5	Flat	13.5

(a) (b)

Fig. 1 *(a) Tapered pin tool; (b) Cylindrical pin Bobbin tool*

2.2 Heat Treatment of Tools

After the machining process, tools were heat treated to increase their hardness from 15 HRC (original hardness) to 40-50 HRC, which is recommended for FSW [34] by using a widely used muffle furnace. In order to prevent decarburization phenomena on tools during the heat treatment process, the tools were first packed in 0.05mm thick stainless steel foil which was closed tightly by wire of mild steel as shown in Fig. **2**(a). A piece of Kraft paper was also placed inside the packet because of its burning capability at elevated temperatures to eliminate the oxygen that is already present inside the packet. Heat treatment process was then carried out on the packet by using a muffle furnace as per designed Thermal cycle, shown in Fig. **2** (b). This process was designed and carried out after an extensive literature review [35,36]. The average tool hardness achieved after this process was 49 HRC.

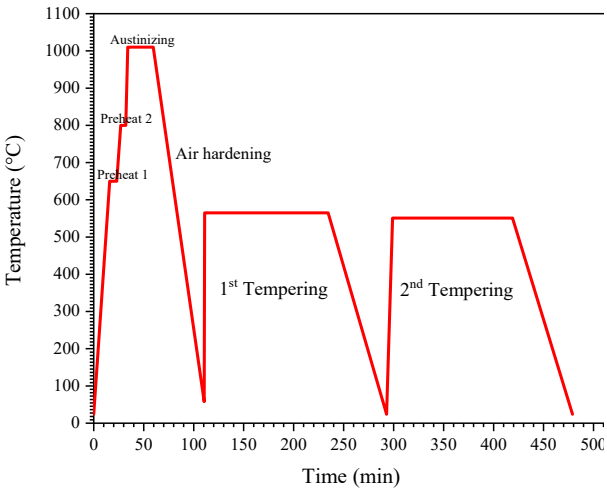

(a) (b)

Fig. 2 *(a) Heat treatment packet; (b) Heat treatment thermal cycle*

2.3 Welding Process

Both CFSW and BFSW were carried out using a conventional universal milling machine which is widely used in industries. The parameters of the experiment are summarized in Table 3. These parameters were decided after reviewing multiple studies [24-34], considering prior experience and machine limitations, to achieve optimal results. A total of two butt joints were fabricated by each technique as shown in Fig. 3 and Fig. 4, the samples were labeled as C1 and C2 for CFSW while BFSW were labeled as B1 and B2.

Table 3 *Working parameters*

Parameters	CFSW		BFSW	
Designation	C1	C2	B1	B2
Rotational Speed (RPM)	670	670	670	950
Transverse Speed (mm/min)	100	100	150	105
Tilt Angle (°)	0°	3°	0°	0°
Tool depth (mm)	3	3	N/A	N/A

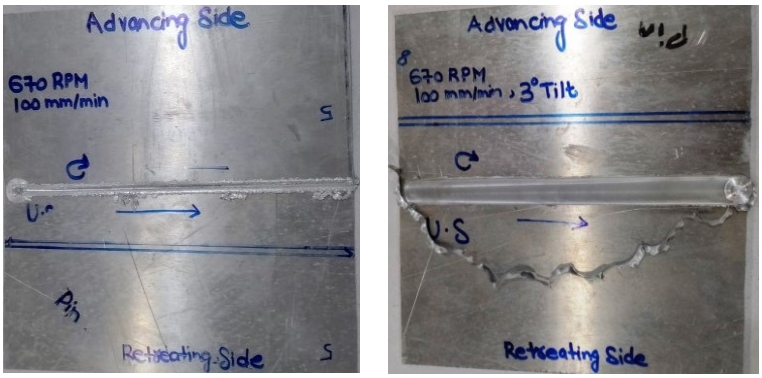

(a) **(b)**

Fig. 3 *Weld achieved by CFSW (a) C1; (b) C2*

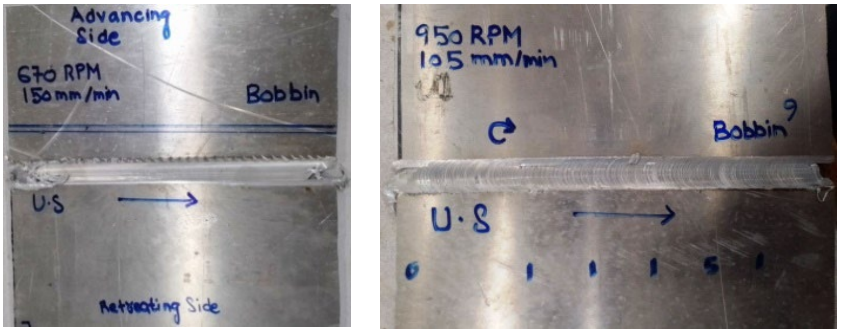

(a) **(b)**

Fig. 4 *Weld achieved by BFSW (a) B1; (b) B2*

2.4 Testing of Joints

The internal defects in the nugget zone (NZ) were analyzed by using X-ray radiography technique. For other observations welded plates of C2 & B2 were sectioned transversely to the weld zone into seven strips, each to form three sets. Two sets had strips from the initial (near starting point of weld), middle and terminal (near endpoint of weld) areas of each plate and a strip of base metal. The first set was used to obtain Microhardness, Microstructures and Macrostructure of zones, for the surface analysis of the weld by consecutively completing the processes of metallography, which include grinding using sandpapers of grit 180, 220, 320, 400 and 600, then polishing by 1µm and 0.05 µm Alumina polishing solution and etching. A solution of 15g NaOH (Sodium hydroxide) in 100ml distilled water was used as an etchant for macrostructures. Keller's regent was the etchant for microstructure and no etching was needed for Microhardness. Moreover, the Vickers microhardness profiles were obtained by applying a load of 200 g with 10s of dwell time, using a Wolpert 402 MVD microhardness tester as per ASTM E384-22. The Second set of strips (i.e., three specimens from the C2 plate and three from the B2 plate) were used to analyze ultimate tensile strength (UTS) according to standard ASTM E8. The Third set had strips from the initial and terminal area of both plates (i.e., a total of four specimens) which were used to perform the Three-point bend test. The dimensions in millimeter scale for Tensile test specimen are shown in Fig. 5.

Fig. 5 *Dimensions of tensile test specimen*

3. Results and Discussion

3.1 X-ray Radiography

Radiograph test was carried out as per ASTM E1742/E1742M all samples. The radiographic result of C1 in Fig. 6(a) shows a dark line oriented in the direction of the weld seam along the weld preparation area which concludes that there is a lack of fusion. It is a condition where the weld tool does not properly fuse the base metal. This happened due to improper penetration of weld tool and absence of tilt angle. A sound and smooth weld was observed in C2 when 3° tilt angle was applied, as no internal defects were observed in radiograph, as shown in Fig. 6(b).

Tunnel defect with the lack of fusion was observed in radiograph of B1 as shown in Fig. 6(c). The tunnel defects generally appear when the traverse speed is high with respect to the rotational speed [37,38]. The undercut defects were observed in B2 along with a small cavity located at 4 inches (101.6 mm), observed in Fig. 6(d). Since it can be seen that joints of C1 & B1 are weak, so only C2 & B2 were considered for further testing.

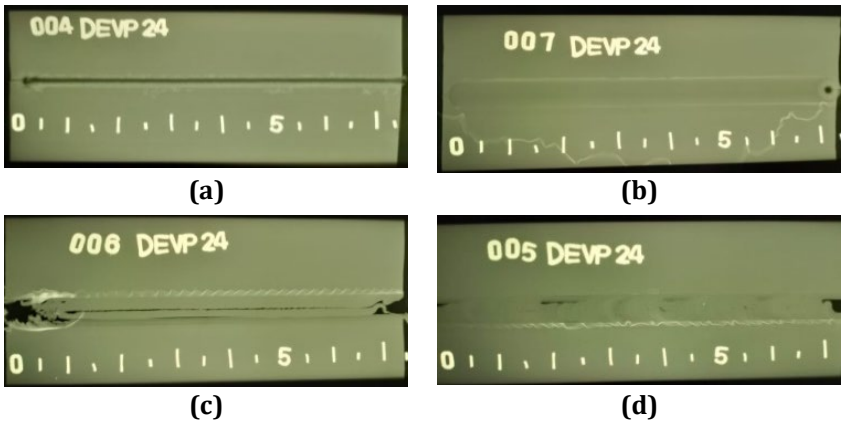

Fig. 6 *Radiographs of (a) C1; (b) C2; (c) B1; (d) B2*

3.2 Microstructure

The Microstructure of Base metal is shown in Fig. 7. There is the presence of Mg_2Si as a black second phase in Fe_3SiAl_{12} gray subscript phase [39]. Mg_2Si phase is more finely distributed in all NZs as shown in Fig. 8a to Fig. 13a.

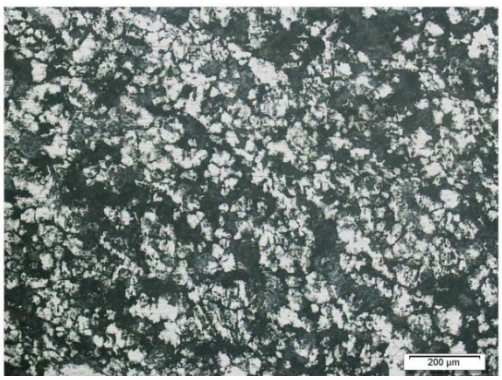

Fig. 7 *Microstructure of Base metal*

J. of Sustainable Materials Processing and Management Vol. 5 No. 1 (2025) p. 76-88

In Thermo Mechanically Affected Zone (TMAZ) as seen in Fig. 8 to Fig. 13b, due to plastically joining of material in NZ. Bent and Elongated grains can be observed in TMAZ because the rolled structure of plates is affected by mechanical rotation of tool which causes the shearing effect. In C2's NZ, plenty of non-hardening Mg2Si (black precipitates) can be found. This explains the reduced hardness in the hardness profile using microhardness shown in Fig. 15. Similarly, microstructures with less black precipitate are found to have more hardness as confirmed by microhardness test.

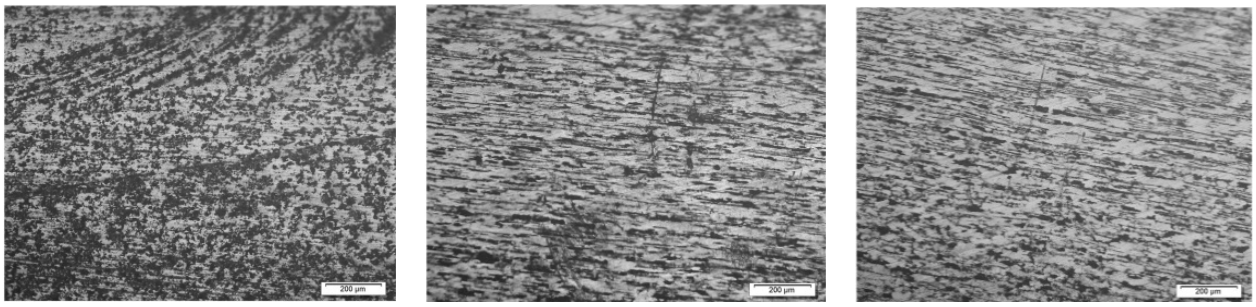

(a) **(b)** **(c)**

Fig. 8 *Microstructure of C2 from sample taken from starting side of weld (a) NZ; (b) TMAZ; (c) BM*

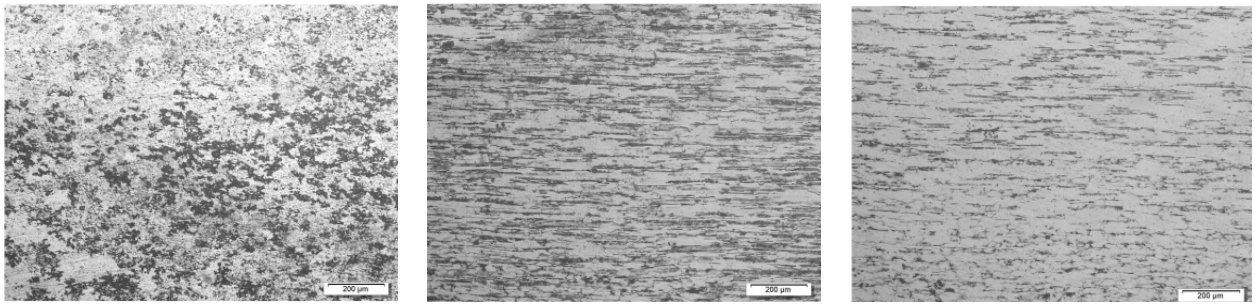

(a) **(b)** **(c)**

Fig. 9 *Microstructure of C2 from sample taken from middle area of weld (a) NZ; (b) TMAZ; (c) BM*

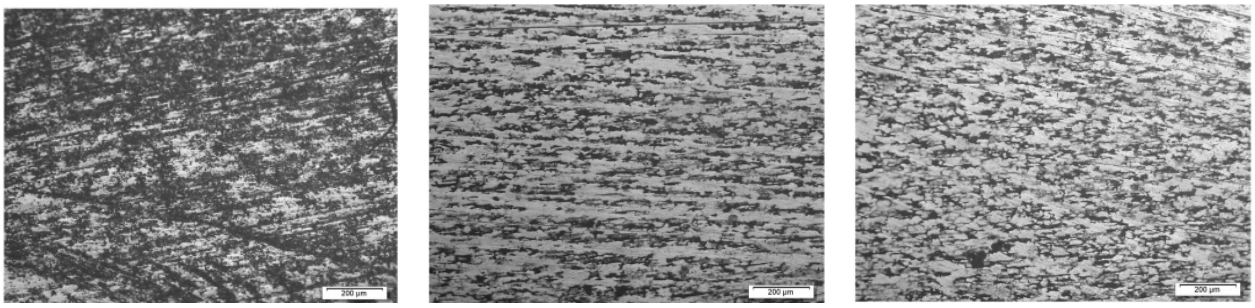

(a) **(b)** **(c)**

Fig. 10 *Microstructure of C2 from sample taken from near end point of weld (a) NZ; (b) TMAZ; (c) BM*

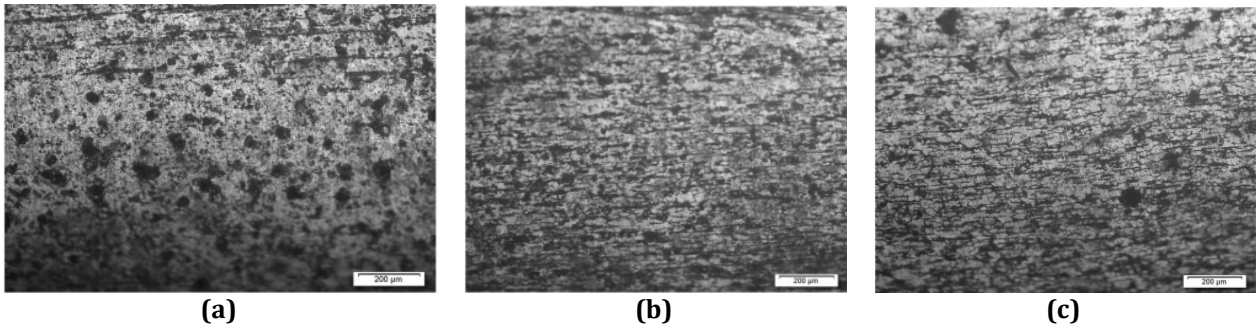

(a) **(b)** **(c)**

Fig. 11 *Microstructure of B2 from sample taken from starting side of weld (a) NZ; (b) TMAZ; (c) BM*

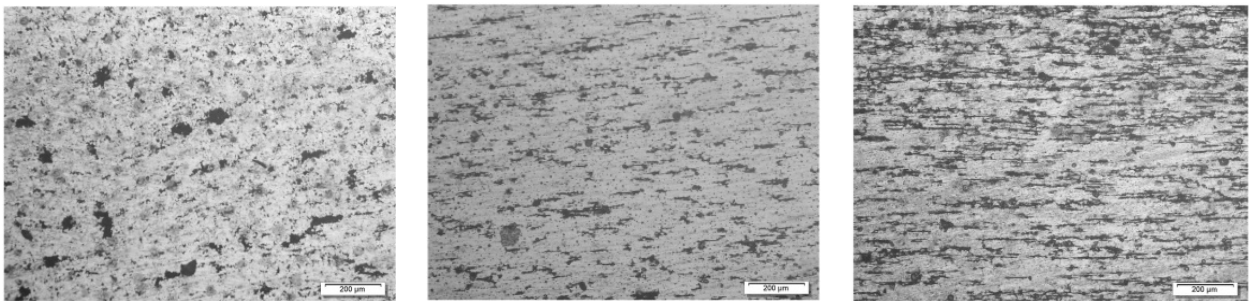

(a) (b) (c)

Fig. 12 *Microstructure of B2 from sample taken from middle area of weld (a) NZ; (b) TMAZ; (c) BM*

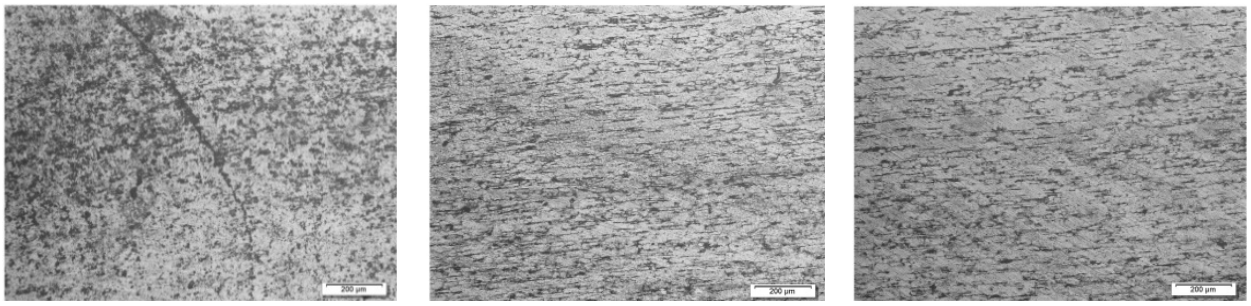

(a) (b) (c)

Fig. 13 *Microstructure of B2 from sample taken from near end point of weld (a) NZ; (b) TMAZ; (c) BM*

3.3 Macrostructure

The observations from cross-sectional macrostructural examination of nugget zones are summarized in Table 4. It can be observed that there is no cavity or hole in C2 weld as there is in B2. Moreover, the NZ of C2 weld has Smooth and fine onion ring morphology which can be observed in Fig. 14(a) and the NZ of B2 weld has rough and coarse onion ring morphology. It can also be observed in micrographs of C2 that the weld top surface is not straight as in B2 weld, which concludes that C2 weld contains an inherent defect of CFSW which is weld thinning. Weld thinning phenomena can weaken the joint due to stress concentration. It is induced by plunge depth of shoulder and is directly related to ribbon flash defect that occurs in welds [19]. Another inherent defect i.e. Keyhole defect in C1 and C2 weld can also be observed in Fig. 3.

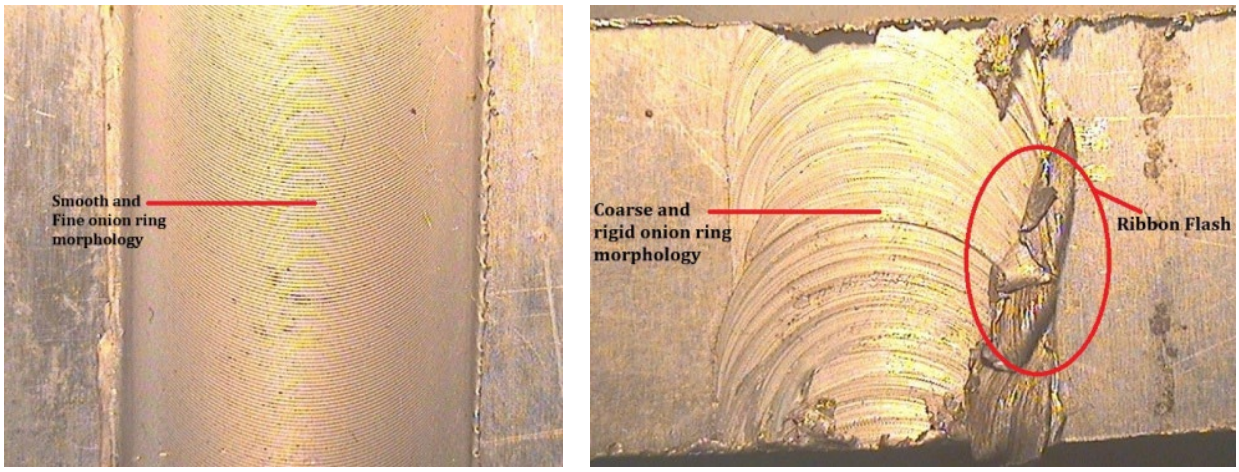

(a) (b)

Fig. 14 *Morphology of NZ in (a) C2; (b) B2*

J. of Sustainable Materials Processing and Management Vol. 5 No. 1 (2025) p. 76-88

Table 4 *Summary of macrostructural examinations*

Weld (Sample position)	Macrograph	Weld Defects	Probable Reasons
C2 (Initial)		Flash	High heat input or high plunge depth [40].
C2 (middle)		Flash	
C2 (terminal)	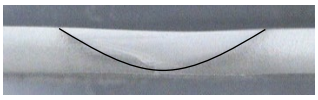	No defects	-
B2 (initial)	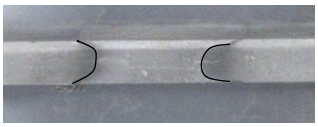	No defects	-
B2 (middle)	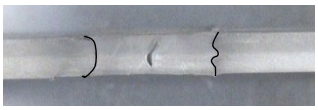	Worm hole at the middle	High tool transverse speed to rotational speed ratio [38].
B2 (terminal)	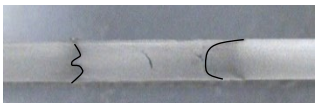	Worm hole	

3.4 Microhardness

The Microhardness tests were performed cross-sectionally at the middle of the plates with equal intervals of 3mm on each side from the center of NZ. The hardness profile of C2 is shown in Fig. 15. At Nugget Zone the highest hardness observed is 73HV (on middle sample), which is 73% of the average base metal.

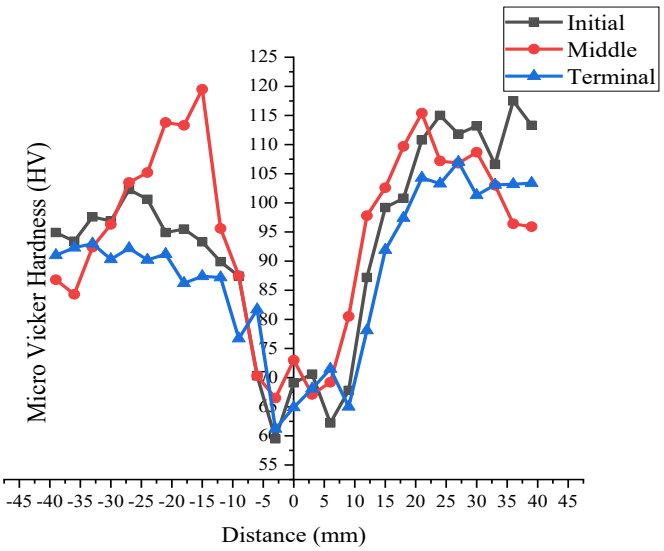

Fig. 15 *Hardness profile of plate welded by C2*

Similarly, the hardness profile of B2 is shown in Fig. 16. The highest hardness in the NZ was observed in the terminal sample 97.1HV i.e. 97.1% of the average base metal hardness. It can be observed that the hardness achieved by B2 is more than C2. Furthermore, in case of B2 the length of NZ is directly proportional to the Hardness achieved.

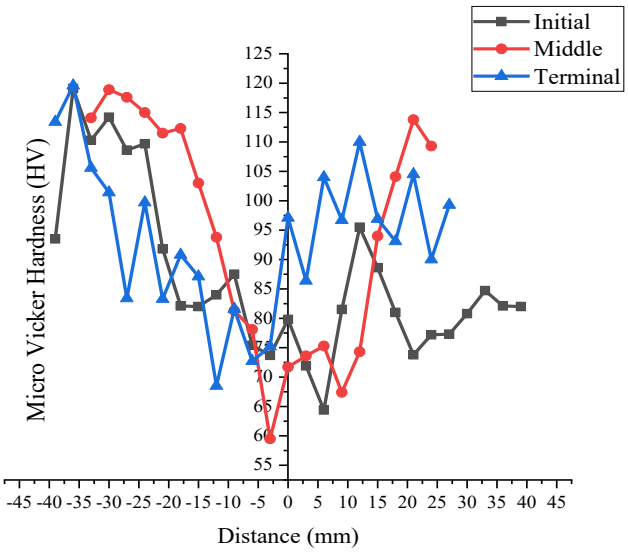

Fig. 16 *Hardness profile of plate welded by B2*

3.5 Tensile Test

The observations conducted from Tensile tests are shown in Fig. 17. Average tensile strength achieved by C2 was found to be 127.2 MPa, including the highest strength of 145.9 MPa observed from the specimen taken from initial part of weld. Similarly, the average tensile strength achieved by B2 was found to be 128 MPa, including the highest strength of 157.6 MPa observed from the specimen taken from middle part of weld. This shows that the average efficiency of weld in in C2 and B2 was 44.8% and 45.1% respectively. Furthermore, it can be observed in Fig. 17 that the tensile strength of B2 becomes greater than that of C2 as the length of nugget zone increases.

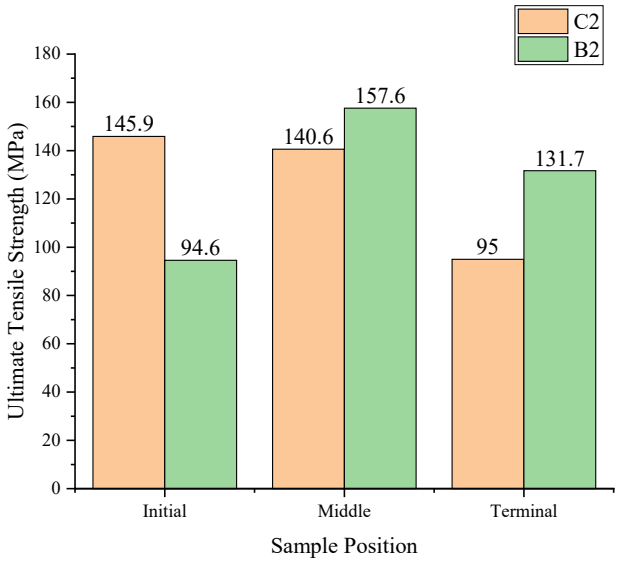

Fig. 17 *Tensile strength of C2 and B2 at different positions of weld*

Similar behavior can be observed in case elongation as shown in Fig. 18. The highest elongation 27.05% and 44.5% was observed in specimen taken from the middle of the weld in both C2 and B2 respectively, which is way more than the elongation observed in base metal (14.2%). This concludes that the joints are ductile in nature.

J. of Sustainable Materials Processing and Management Vol. 5 No. 1 (2025) p. 76-88

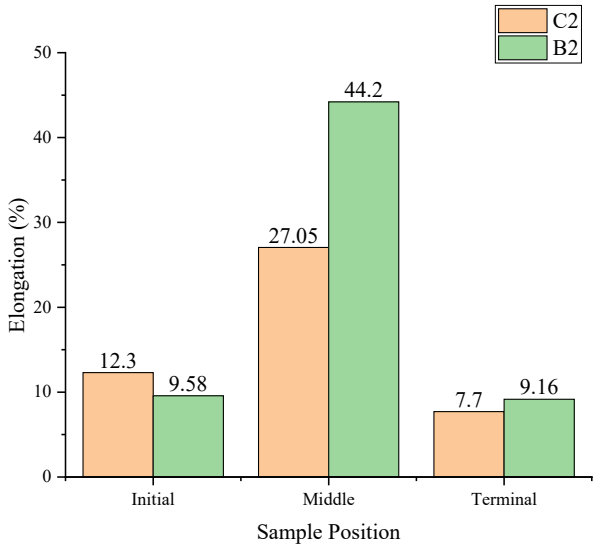

Fig. 18 *Elongation % of C2 and B2 at different positions of weld*

3.6 Bend Test

Fig. 19 shows three-point bend test results. It was observed that C2 joint had more bend strength than B2. Furthermore, in case of B2 joint, the bend strength is found to be increasing along the length of NZ. Whereas in case of C2 joint, it decreases as the length of NZ increases.

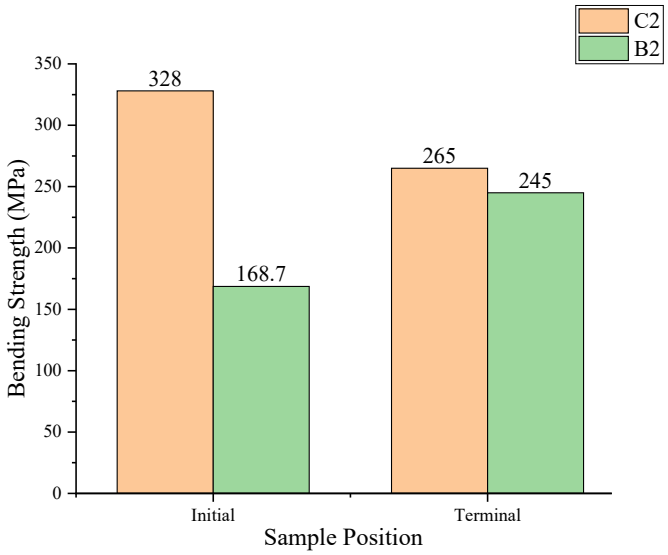

Fig. 19 *Bending strength of C2 and B2 at different positions of weld*

4. Conclusion

The following important conclusions can be drawn by this comparative investigation of CFSW and BFSW:

- Among the two butt joints fabricated by CFSW, the joint with a 3° tilt angle parameter was a defect-free and strong joint, as C2 was found to be a sound and smooth weld in the X-ray radiography test.
- Among the joints fabricated by BFSW, the joint fabricated under parameters of 950rpm rotational speed and 105mm/min transverse speed was found to be more defect-free and stronger joint by X-ray radiography testing.
- The microstructural investigation showed that the formation of non-hardening Mg_2Si (black precipitates) is more in the NZ of CFSW as compared to BFSW. This resulted in greater hardness retention by BFSW joint than CFSW as confirmed by microhardness testing.

- The Tensile and Bend test revealed that as the length of (NZ in) joint increases, the mechanical properties achieved by the BFSW joint increased as compared to CFSW. This concluded that BFSW is a better option for longer joints.
- The 'T6' tempering effect was observed to be retained in the joints, as they exhibited ductile behavior during the elongation study in the tensile test and showed hardness values close to the base metal (6061-T6) in the microhardness test.

Acknowledgement

This research is carried out under HEC Pakistan funded NRPU-17040. The authors are thankful to the Department of Materials Engineering and Department of Industrial & Manufacturing Engineering, NED University of Engineering and Technology for their support in experimental work. Special thanks to Dr. Amir Iqbal and Dr. Muhammad Wasif for their valued feedback during various stages of the project.

Conflict of Interest

Authors declare that there is no conflict of interests regarding the publication of the paper.

Author Contribution

The authors confirm contribution to the paper as follows: ***study conception and design:*** *Rawaha Imran Elahi, Muhammad Sohail Hanif, Syed Ahsan Abbas Zaidi, Muhammad Taha Siddiqui;* ***data collection:*** *Rawaha Imran Elahi, Syed Ahsan Abbas Zaidi, Muhammad Taha Siddiqui, Bilal Ahmed;* ***analysis and interpretation of results:*** *Rawaha Imran Elahi, Syed Ahsan Abbas Zaidi, Muhammad Taha Siddiqui, Bilal Ahmed;* ***draft manuscript preparation:*** *Rawaha Imran Elahi, Muhammad Sohail Hanif. All authors reviewed the results and approved the final version of the manuscript.*

References

[1] Thomas, W.M., Nicholas, E.D., Needham, J.C., Murch, M.G., Templesmith, P. and Dawes, C.J. (1991) International Patent Application No. PCT/GB92/02203 and GB Patent Application No. 9125978.8.
[2] Sato, S., Enomoto, M., Kato, R., & Uchino, K. (1998). Application of aluminum extrusions to suspension arms (No. 982331). SAE Technical Paper. p. 8. https://doi.org/10.4271/982331
[3] Kallee, S. W. (2010). *Industrial applications of friction stir welding*. In Friction stir welding (pp. 118-163). Woodhead Publishing. https://doi.org/10.1533/9781845697716.1.118
[4] Dawes, C. J. (1995). An introduction to friction stir welding and its development. *Welding & Metal Fabrication*, 63, 13-16.
[5] Lohwasser, D., & Chen, Z. (Eds.). (2009). *Friction stir welding: From basics to applications*. Elsevier.
[6] Johnson, R., & Kallee, S. (1999). Stirring stuff from friction welding. *Materials world*, 7(12), 751-753.
[7] Oosterkamp, A. A. N. A. (2004). Kissing bond" phenomena in solid-state welds of aluminum alloys. *The welding Journal*, 83, 225-231.
[8] Fathi, J., Ebrahimzadeh, P., Farasati, R., & Teimouri, R. (2019). Friction stir welding of aluminum 6061-T6 in presence of watercooling: Analyzing mechanical properties and residual stress distribution. *International Journal of Lightweight Materials and Manufacture*, 2(2), 107-115. https://doi.org/10.1016/j.ijlmm.2019.04.007
[9] Swarnkar, A., Kumar, R., Suri, A., & Saha, A. (2016, December). A review on Friction Stir Welding: An environment friendly welding technique. In *2016 IEEE Region 10 Humanitarian Technology Conference (R10-HTC)*, pp. 1-4. https://doi.org/10.1109/R10-HTC.2016.7906807
[10] Sued, M. K., Pons, D., Lavroff, J., & Wong, E. H. (2014). Design features for bobbin friction stir welding tools: Development of a conceptual model linking the underlying physics to the production process. *Materials & Design (1980-2015)*, 54, 632-643. https://doi.org/10.1016/j.matdes.2013.08.057
[11] Hilgert, J., Schmidt, H. N. B., Dos Santos, J. F., & Huber, N. J. J. M. P. T. (2011). Thermal models for bobbin tool friction stir welding. *Journal of Materials Processing Technology*, 211(2), 197-204. https://doi.org/10.1016/j.jmatprotec.2010.09.006
[12] Schmidt, H., & Hattel, J. (2005). Modelling heat flow around tool probe in friction stir welding. *Science and Technology of Welding and joining*, 10(2), 176-186. https://doi.org/10.1179/174329305X36070
[13] Mishra, R. S., & Ma, D. Z. (2005). Friction stir welding and processing. *Materials science and engineering: R: reports*, 50(1-2), 1-78. https://doi.org/10.1016/j.mser.2005.07.001
[14] Wu, D., Li, W. Y., Gao, Y. J., Yang, J., Su, Y., Wen, Q., & Vairis, A. (2020). Effect of an improved pin design on weld formability and mechanical properties of adjustable-gap bobbin-tool friction stir welded Al-Cu aluminum alloy joints. *Journal of Manufacturing Processes*, 58, 1182-1188. https://doi.org/10.1016/j.jmapro.2020.09.015

[15] Chen, S., Li, H., Lu, S., Ni, R., & Dong, J. (2016). Temperature measurement and control of bobbin tool friction stir welding. The International Journal of Advanced Manufacturing Technology, 86, 337-346. https://doi.org/10.1007/s00170-015-8116-9
[16] Tinguery, K. M. S., Rahem, A., Nadeau, F., & Fafard, M. (2023). Friction stir welding parameters development of aa6061-t6 extruded alloy using a bobbin tool. *Engineering proceedings*, 43(1), 50. https://doi.org/10.3390/engproc2023043050
[17] Salari, E., Jahazi, M., Khodabandeh, A., & Ghasemi-Nanesa, H. (2014). Influence of tool geometry and rotational speed on mechanical properties and defect formation in friction stir lap welded 5456 aluminum alloy sheets. Materials & Design, 58, 381-389. https://doi.org/10.1016/j.matdes.2014.02.005
[18] Ghangas, G., & Singhal, S. (2018). Effect of tool pin profile and dimensions on mechanical properties and microstructure of friction stir welded armor alloy. Materials Research Express, 5(6), 066555. https://doi.org/10.1088/2053-1591/aacdb1
[19] Meng, X., Huang, Y., Cao, J., Shen, J., & dos Santos, J. F. (2021). Recent progress on control strategies for inherent issues in friction stir welding. *Progress in Materials Science*, 115, 100706. https://doi.org/10.1016/j.pmatsci.2020.100706
[20] Van Huis, M. A., Chen, J. H., Zandbergen, H. W., & Sluiter, M. H. F. (2006). Phase stability and structural relations of nanometer-sized, matrix-embedded precipitate phases in Al–Mg–Si alloys in the late stages of evolution. *Acta Materialia*, 54(11), 2945-2955. https://doi.org/10.1016/j.actamat.2006.02.034
[21] Yao, J. Y., Graham, D. A., Rinderer, B., & Couper, M. J. (2001). A TEM study of precipitation in Al–Mg–Si alloys. *Micron*, 32(8), 865-870. https://doi.org/10.1016/S0968-4328(00)00095-0
[22] Troeger, L. P., & Starke Jr, E. A. (2000). Microstructural and mechanical characterization of a superplastic 6xxx aluminum alloy. *Materials Science and Engineering: A*, 277(1-2), 102-113. https://doi.org/10.1016/S0921-5093(99)00543-2
[23] Chen, J. H., Costan, E., Van Huis, M. A., Xu, Q., & Zandbergen, H. W. (2006). Atomic pillar-based nanoprecipitates strengthen AlMgSi alloys. Science, 312(5772), 416-419.
[24] Hoyos, E., & Serna, M. C. (2021). Basic tool design guidelines for friction stir welding of aluminum alloys. *Metals*, 11(12), 2042. https://doi.org/10.3390/met11122042
[25] Chupradit, S., Bokov, D. O., Suksatan, W., Landowski, M., Fydrych, D., Abdullah, M. E., & Derazkola, H. A. (2021). Pin angle thermal effects on friction stir welding of AA5058 aluminum alloy: CFD simulation and experimental validation. *Materials*, 14(24), 7565. https://doi.org/10.3390/ma14247565
[26] Fuse, K., & Badheka, V. (2021). Effect of shoulder diameter on bobbin tool friction stir welding of AA 6061-T6 alloy. Materials Today: Proceedings, 42, 810-815. https://doi.org/10.1016/j.matpr.2020.11.366
[27] Amin, S. A., Hanna, M. Y., & Mohamed, A. F. (2018). Experimental study the effect of tool design on the mechanical properties of bobbin friction stir welded 6061-T6 aluminum alloy. *Al-Khwarizmi Engineering Journal*, 14(3), 1-11. https://doi.org/10.22153/kej.2018.01.003
[28] Liu, H. J., Hou, J. C., & Guo, H. (2013). Effect of welding speed on microstructure and mechanical properties of self-reacting friction stir welded 6061-T6 aluminum alloy. *Materials & Design*, 50, 872-878. https://doi.org/10.1016/j.matdes.2013.03.105
[29] Amin, S. A., Hanna, M. Y., & Mohamed, A. F. (2018). Modeling and optimization of bobbin friction stir welding for AA6061-T6 alloy utilizing response surface methodology. *Journal of University of Babylon for Engineering Sciences*, 26(4), 1-17.
[30] Patel, J. B., & Patil, H. S. (2014). Simulation of peak temperature & flow stress during FSW of aluminium alloy AA6061 for various tool pin profiles. *Int J Mater Sci Eng*, 2(1), 67-71. https://doi.org/10.12720/ijmse.2.1
[31] Garg, A., Raturi, M., & Bhattacharya, A. (2020). Strength, failure and microstructure development for friction stir welded AA6061-T6 joints with different tool pin profiles. *CIRP Journal of Manufacturing Science and Technology*, 29, 99-114. https://doi.org/10.1016/j.cirpj.2020.03.001
[32] Safeen, W., Hussain, S., Wasim, A., Jahanzaib, M., Aziz, H., & Abdalla, H. (2016). Predicting the tensile strength, impact toughness, and hardness of friction stir-welded AA6061-T6 using response surface methodology. *The International Journal of Advanced Manufacturing Technology*, 87, 1765-1781. https://doi.org/10.1007/s00170-016-8565-9
[33] Kang, S. H, Cha, J. H., & Kang, M. J. (2021). A Review on the Design Rule for the Friction Stir Welding using Bobbin Tool for Aluminum. *Journal of Welding and Joining*, 39(5), 520-526. https://doi.org/10.5781/JWJ.2021.39.5.8
[34] Rajakumar, S., Muralidharan, C., & Balasubramanian, V. (2011). Predicting tensile strength, hardness and corrosion rate of friction stir welded AA6061-T6 aluminium alloy joints. *Materials & Design*, 32(5), 2878-2890. https://doi.org/10.1016/j.matdes.2010.12.025
[35] Bryson, W. E. (2005). Heat treatment, selection, and application of tool steels. Heat Treatment, Selection, and Application of Tool Steels, I-XV. *Hanser Publications.*

[36] Akhtar, S. S., Arif, A. F. M., Yilbas, B. S., & Sheikh, A. K. (2010). Influence of surface preparation on the kinetics of controlled gas-nitrided AISI H13 steels used in extrusion dies. *Journal of Materials Engineering and performance*, 19, 347-355. https://doi.org/10.1007/s11665-009-9496-5
[37] Khan, N. Z., Siddiquee, A. N., Khan, Z. A., & Shihab, S. K. (2015). Investigations on tunneling and kissing bond defects in FSW joints for dissimilar aluminum alloys. *Journal of alloys and Compounds*, 648, 360-367. https://doi.org/10.1016/j.jallcom.2015.06.246
[38] Nandan, R., DebRoy, T., & Bhadeshia, H. K. D. H. (2008). Recent advances in friction-stir welding–process, weldment structure and properties. *Progress in materials science,* 53(6), 980-1023. https://doi.org/10.1016/j.pmatsci.2008.05.001
[39] Vander Voort, G.F. (2004). Metallography and microstructures, asm handbook. *ASM International.*
[40] Kim, Y. G., Fujii, H., Tsumura, T., Komazaki, T., & Nakata, K. (2006). Three defect types in friction stir welding of aluminum die casting alloy. Materials Science and Engineering: A, 415(1-2), 250-254. https://doi.org/10.1016/j.msea.2005.09.072